ISSN 1068-1620, Russian Journal of Bioorganic Chemistry, 2012, Vol. 38, No. 2, pp. 152–158. © Pleiades Publishing, Ltd., 2012.
Original Russian Text © O.S. Sokolova, K.V. Shaitan, A.V. Grizel, A.V. Popinako, M.G. Karlova, M.P. Kirpichnikov, 2012, published in Bioorganicheskaya Khimiya, 2012, Vol. 38, No. 2, pp. 177–184.

Three-Dimensional Structure of Human Voltage-Gated Ion Channel Kv10.2 Studied by Electron Microscopy of Macromolecules and Molecular Modeling

O. S. Sokolova[a, b, 1], K. V. Shaitan[a], A. V. Grizel[a], A. V. Popinako[a], M. G. Karlova[a], and M. P. Kirpichnikov[a]

[a] *Moscow State University, Biology Department, Moscow, 119991 Russia*
[b] *Institute of Crystallography, Russian Academy of Sciences, Moscow, 119333 Russia*

Received June 27, 2011; in final form, August 17, 2011

Abstract—Three-dimensional structure of the human voltage-gated channel Kv10.2 has been elucidated for the first time using the method of electron microscopy with 2.5 nm resolution. The molecule has a distinct domain structure. For interpretation of the structure, homology modeling was used with the cAMP-dependent channel MlotiK1 (C-subunit) structure used as a template for a membrane part of the channel, homology with the structure of the human potassium channel *herg* (A subunits) was used for the cytoplasmic subdomains PAS-PAC, and for the cNBD domain homology with the MloK1 channel was used. The homologous transmembrane part corresponds by size to the upper part of the three-dimensional reconstruction. Cytoplasmic domains of the Kv10.2 channel form the structure built according to the 'hanging gondola' type that is connected with the transmembrane part of the channel by linkers. The length of linkers suggests the possibility of contacts between the C-terminal cNBD domains and N-terminal PAS-domains.

Keywords: ion channels; heag2; electron microscopy; molecular modeling
DOI: 10.1134/S1068162012020100

INTRODUCTION

Potassium channels play a critical role in the function of excitable cells including the maintenance of the transmembrane potential, membrane re-polarization, and the emergence of an action potential. They also are the cause for the widespread pathologies and many inheritable diseases in particular [1]. The correct functioning of potassium channels is vital for the neurotransmitters and hormone secretion and support of heart function. Convincing data exist that show natural changes occur in the gene expression of some potassium channels during the malignant cell transformation, and this correlates with the cell ability for uncontrolled growth and metastasis [2].

Data on the three-dimensional structure of ion channels are necessary for understanding the mechanism of action and activity changes. Detailed study of activation/inactivation mechanisms of the channel is possible if the three-dimensional structure is known through, for example, methods of molecular modeling, to enable planning of experiments on directed mutagenesis and new drug design.

Currently, many genes encoding eukaryote ion channels and their bacterial analogues are cloned. However, the quaternary structure is unknown for the majority of ion channels as they are difficult to crystallize. Researchers were able to elucidate the entire structure of several prokaryote (for example [3, 4]) and eukaryote channels [5–10]. Extramembranous parts of the protein (N- and C-termini as a rule) complicate crystallization due to their flexibility. Protein that does not have large cytoplasmic domains (as in [3, 9]) or N- and C-terminal truncated protein (as in [10]) are often used for crystal formation. At the same time, the combination of electron microscopy of macromolecules and molecular modeling approaches presents a unique opportunity to investigate the structure of full-sized channels.

The recently discovered human voltage-gated channel *heag2* [11] belongs to the family of ether-a-go-go (according to the accepted nomenclature Kv10) [12]. It is localized mainly in brain, but is found in other tissues [13–15]. It has been shown that the *heag2* is connected with the processes of tumor emergence and development [16]. Overexpression of this channel has been discovered in many tumor types, and its inhibition led to the decline of cancer cell proliferation

Abbreviations: Kv, voltage-gated potassium channel; cAMP, cyclic adenosine monophosphate; 3D, three-dimensional image; FS, three-dimensional Fourier shell correlation; CCD, Charge Coupled Device; MSA, multivariate statistical analysis; MRA, multi-reference analysis; PAAG, polyacrylamide gel.

[1] Corresponding author: phone: + 7 (495) 938-00-05; fax: +7 (495) 939-57-38; e-mail: sokolova@mail.msu.ru.

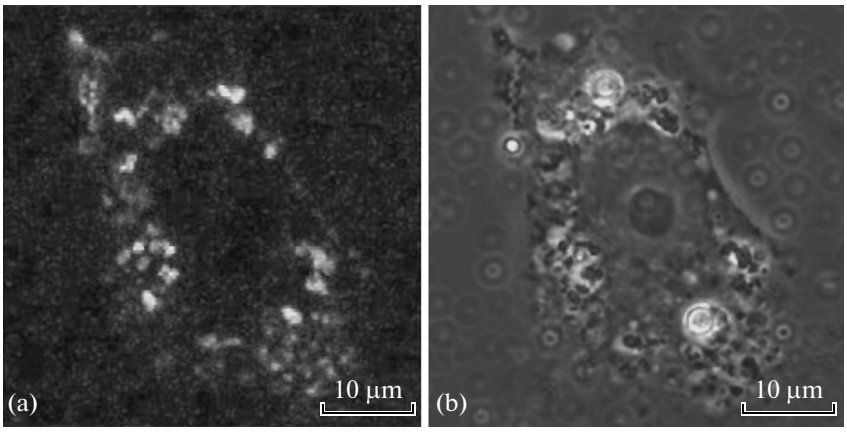

Fig. 1. Expression of the Kv10.2 (*heag2*) ion channels on the surface of cells investigated by fluorescence method. (a) The distribution of the fluorescence of agitoxin labeled with the Cy-3 dye on the surface of Vero cells; (b) Cells in the transmitted light corresponding to the image in (a).

[17], which could be used for the development of new anticancer agents and diagnostic methods. It is known that the massive cytoplasmic terminals of this channel could contain subdomains (PAS and PAC at the N-terminus; domain that supposedly responsible for cAMP binding—cNBD—at the C-terminus).

The aim of this work was expression in eukaryotic cells and purification of the full-sized Kv10.2 (*heag2*) ion channel and investigation of its structure by the method of electron microscopy of macromolecules. As a result, the three-dimensional structure of the Kv10.2 channel with 2.5 nm resolution was obtained for the first time. Folding of the expressed channel was tested using a neurotoxin from scorpion venom. Homology modeling using the known crystal structures of channels and separate domains was used for the interpretation of the three-dimensional structure obtained.

RESULTS AND DISCUSSION

Channels of the Kv10 family structurally differ from the proteins of other families of voltage-gated potassium channels [12]. They have the PAS-domain at the N-terminus, and the C-terminus part is structured with the formation of the cNBD-domain. The atomic structure of the PAS-domain of the homologous *herg* channel of this family is resolved using an X-ray technique [18]. The structure of the cNBD-domain is resolved for the hyperpolarization-activated HCN-channel [19].

Direct structural data for the Kv10.2 channel and location of its cytoplasmic domains that play an important role in the channel functioning [1] are not currently available, probably due to the difficulties of protein crystallization. Hence, the method of electron microscopy of macromolecules [20, 21] was used for determination of the three-dimensional structure of the full-sized human Kv10.2 channel. As a result, the three-dimensional structure of the full-sized human Kv10.2 channels with 2.5 nm resolution was obtained for the first time, and composition domains were also identified.

The protein of Kv10.2 channel (*M* 130 kDa) was expressed in green monkey kidney cells and purified using affinity chromatography as described before [22]. The correctness of folding was confirmed by the method developed earlier using fluorescently labeled agitoxin from scorpion venom [23] (Fig. 1). The method is based on the fact that agitoxin binds with the active Kv channels in the stochiometric ratio of 1 : 1 [24]. Western blot confirmed the protein expression in the extract of transfected cells (Fig. 2).The observed bands of different molecular mass indicated *N*-glycosylation, which is characteristic for the homologous channel Kv10.1 [25]. It is known that the protein homology between Kv10.1 and Kv10.2 is 73%, and glycosylated amino acids are fully identical [11]. Protein

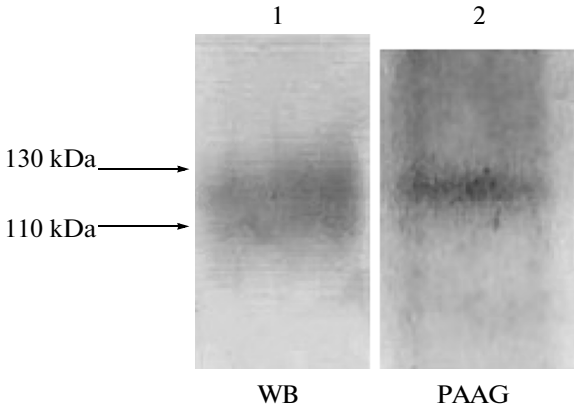

Fig. 2. Purification of Kv10.2 channel protein. Lanes: 1, Western blot of the eluate from the BrCN-agarose column; 2, gel-electrophoresis in PAAG.

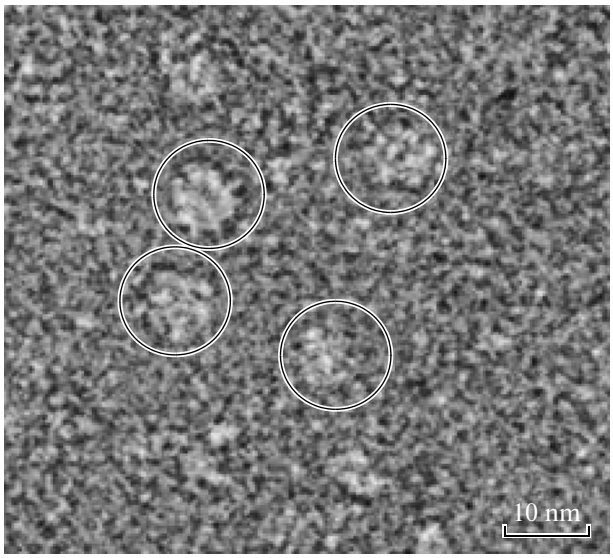

Fig. 3. Micrograph of the channels stained with uranyl acetate. The separate molecules marked with white circles. Scale bar, 10 nm.

electrophoresis in PAAG followed by the gel staining with silver nitrate confirmed the purity of the protein after purification on the affinity column (Fig. 2). As a result, a sufficient amount of the purified Kv10.2 channel protein was obtained to investigate its structure by the method of electron microscopy of macromolecules using negative staining with heavy metal salts. Electron micrographs with clear images of the individual channel molecules are presented in Fig. 3.

The images of individual molecules were collected and processed by the computer using the procedures of classification and alignment, which were followed by computation of the three-dimensional model of the full-sized human voltage-gated channel Kv10.2 (Fig. 4). The contour level chosen for the three-dimensional structure visualization was based on the average protein density data equaled to 810 Da/nm^3 and molecular mass of the protein tetramer ~590 kDa. These data account for carbohydrate component, 1D4 affinity tag, and bound detergent, approximately 15 kDa per subunit [22].

The obtained three-dimensional structure has a trapezoidal shape with ~9.5 nm height, and width in the upper part of ~10, and the lower part, ~12 nm. The upper part of the channel (marked as 'TM' in Fig. 4) has a slight ledge with the diameter of ~3 nm, which we consider being a result of protein *N*-glycosylation. This hypothesis is supported by the availability of a similar ledge on the surface of the membrane domain of the Kv10.1 channel [22], which also is glycosylated.

Since there is no crystal structure for Kv10.2 available, docking of the homologous domain structures (transmembrane domain, PAS-PAC, cNBD) was used for interpretation of the three-dimensional structure of the full-sized channel. Homology modeling using the crystal structures of domains of other ion channels (MlotiK1, N-terminal domain of the human potassium channel *herg*, bacterial cAMP-dependent channel—MloK1) was conducted for this purpose. It is worth noting that the transmembrane part is, as a rule, homologous for all eukaryotic Kv channels (more than 20% homology). The highest homology for the investigated channel corresponded to the structure of the ligand-dependent bacterial channel MlotiK1 that was used as a template for the homology modeling. The model of transmembrane domain obtained corresponded well by size to the upper part of the reconstruction (Fig. 5a), the ledges of which have a cross-like shape with slightly rounded blades. Hence, the upper part of the model is more likely transmembrane and the lower part, cytoplasmic.

The wide cytoplasmic part is divided in subdomains ("P" and "D" in Fig. 4), which are formed by N- and C-terminal domains. The characteristic "windows" are visible between two parts of the channel ("O" in Fig. 4) bounded by linkers. The similar "windows" were observed for majority of the Kv-channel

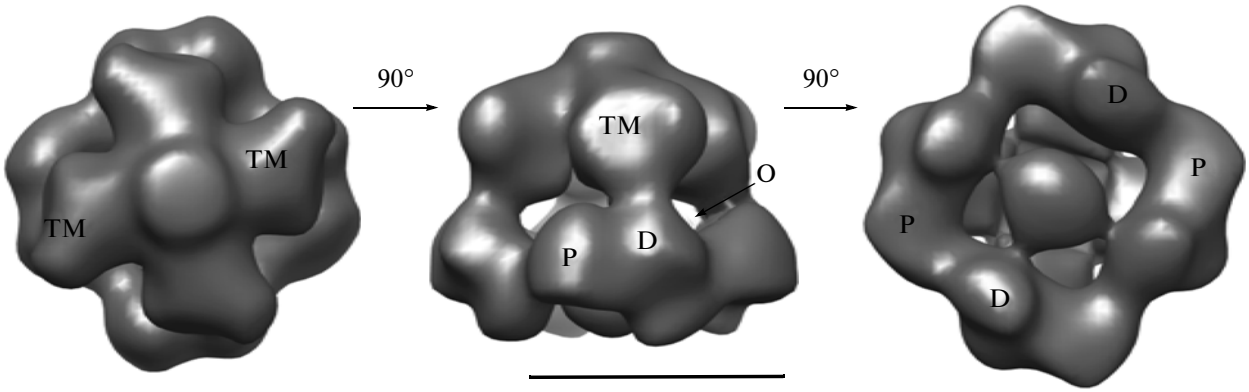

Fig. 4. Three-dimensional reconstruction of the Kv10.2 channel. From left to right: top, side, and bottom views. Scale bar is 10 nm. TM is the membrane domain; P and D, the cytoplasmic domains; O, "window".

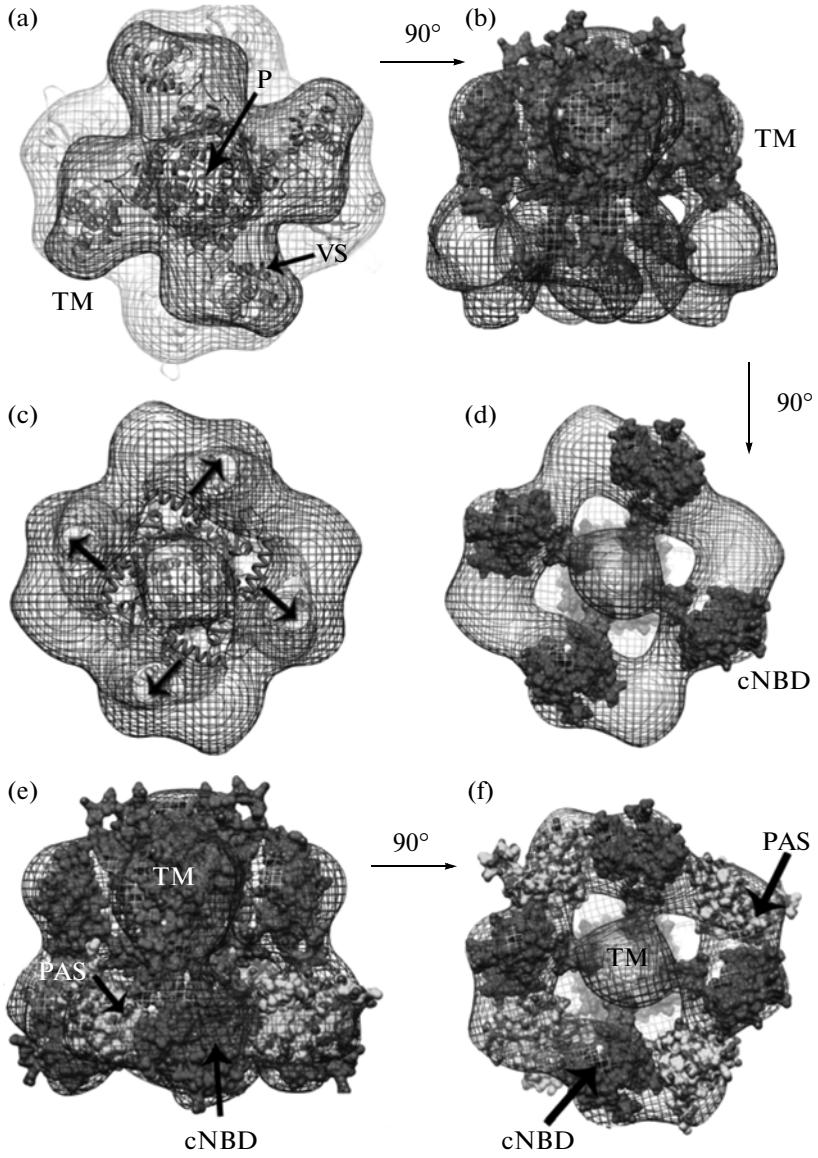

Fig. 5. Interpretation of the Kv10.2 channel reconstruction. (a) Docking of the transmembrane domain in the upper part of Kv10.2 channel reconstruction, top view. TM is the transmembrane domain; P, the channel pore; VS, the voltage-sensor domain; (b), the same, side view; (c), docking of the cNBD-domain tetramer modeled by the homology with the crystal structure of the human cAMP-dependent channel HCN4 (PDB ID: 3OTF), bottom view; (d), the bottom view: docking of the cNBD-domain in the "P" area subdomain; (e), side view: docking of the PAS-PAC domains and cNBD in the cytoplasmic part; (f), bottom view, designations as in Fig. 5e.

structures obtained with low resolution [22, 26–28]; they serve for the channel inactivation by the N-terminal peptides. The sizes of "windows", bounded by linkers, are approximately 0.25 × 0.3 nm^2 in our model, which is in agreement with the previous data for the *Shaker* channel [22].

The docking of several homologous domains of N- and C-terminal domains was conducted to interpret the structure of the cytoplasmic part of the channel (Figs. 5d–5f). Two crystal structures, human cAMP-dependent channel HCN4 crystallized in the presence of AMP (PDB code 3OTF) and bacterial cAMP-dependent channel MloK1 (PDB code 2KXL), were used for the docking of the cNBD domain. Docking of the cNBD tetramer with cAMP resulted in the structure not corresponding to the reconstruction (Fig. 5c). However, the move of a separate monomer in the direction indicated by arrows in Fig. 5c makes it possible to build them into the area of D subdomains. The relative correspondence of volumes of subdomains and cNBD monomers supports this variant (Fig. 5d). Hence, the cNBD domains in the composition of the channel pro-

tein are probably located at a larger distance than in the isolated crystal structure (Figs. 5c, 5d).

Docking of the N-terminal domains (PAS-PAC) in the area of P subdomains results in the placement of these domains farther from the central axis of the channel in direct contact with C-terminal domains (Figs. 5e, 5f). This location corresponds to the earlier hypothesis suggesting the location of the compact cNBD tetramer in the center of the cytoplasmic part of the channel, and PAS-domains in contact with them closer to periphery. The data obtained in the paper refine this hypothesis. The possible re-grouping of the C-terminal domains could be suggested as our structure of the Kv10.2 channel was determined in the absence of ligands.

The interaction with toxin confirmed the correctness of folding in the investigated protein molecules of the channel, which was also illustrated by the successful docking of the tetrameric structure of the transmembrane domain in the upper part of the reconstruction (Figs. 5a, 5b). Docking of the atomic structure of transmembrane domain suggested the location of important structures in the channel composition, such as channel pore and voltage-sensing domains (Fig. 5a) that were indistinguishable at 2.5 nm resolution.

The membrane domain of Kv10.2 channel is distinctive in respect of the availability of non-structure loops both in cytoplasmic and periplasmic areas that do not fit the reconstruction (Fig. 5b). It should be noted, though, that flexible parts of the protein chain are impossible to detect, not only by electron microscope, but by the X-ray method as well. It is worth mentioning also that the fixed sited of the loops in the periplasmic area could partly form the ledge on the extracellular channel surface described above in addition to *N*-glycans. The loops in the cytoplasmic area could form linkers between the transmembrane part and "hanging gondola" formed by the cytoplasmic domains (Fig. 4). The similar structure is characteristic of the majority of investigated potassium channels [6, 22, 26–28]. The so-called "tetramerization" N-terminal domain [22] responsible for the folding is located in the center of "gondola" surrounded by the C-terminal domains in the channels belonging to the families Kv1.x–Kv9.x [27]. Based on the experimental data of scanning mutagenesis and investigation of the PAS-PAC oligomeric state, it was suggested earlier that the N-terminal domain of Kv10 channels is located outside of the C-terminal [1]. The location of this structure relative to the transmembrane domain was unknown.

Interaction between the N-terminal PAS-domains and the transmembrane part of the channel was predicted for the other voltage-gated channels [29–31]. Our data confirmed the availability of linkers between the transmembrane and cytoplasmic parts of the Kv10-channel with the length of approximately 0.1 nm (Fig. 4), which is sufficient for the contact of C-terminal cNBD domains with N-terminal PAS-domains. PAS-domains in our reconstruction are located 0.1 nm closer to the transmembrane part than cNBD domains, which is sufficiently close to interact with S4-S5 linker and by this means to affect the channel deactivation [30, 31].

EXPERIMENTAL

Expression of the voltage-gated channel. Eukaryote cell line of the green monkey kidney from the collection of OOO Biolot (Russia) was used for potassium channel expression. The production of pMT3Kv10.2 was conducted in the TG1 strain. Plasmids for transient eukaryote cell transfection were isolated using HiSpeed Plasmid Maxi kit (QIAGEN, Netherlands).

Vero cells were grown in Petri dishes in DMEM medium containing high glucose content (HyClone, USA) and supplemented with 10% fetal bovine serum. Cells were transfected with pMT3 plasmid encoding the full-sized Kv10.2 channel using Metafecten™ PRO transfection agent (Biontex, Bulgaria) according to manufacturer instructions.

For confocal microscopy cells were grown on the round 24-mm coverslips in the 6-well plates (30×10^3 cells per well) for 22–24 h in 2 mL of medium (see above) followed by the transient transfection. The medium was changed for the fresh 24 h after transfection. The expression level of channel proteins was tested after 48 h of growth using labeled agitoxin [23].

Purification of the voltage-gated potassium channel protein. Cells were cultivated for 48 h after transfection, washed by the cold PBS-buffer with pH 7.4, scraped from the dish surface and frozen at –80°C for further use. The protein purification was performed using affinity chromatography on the activated BrCN-agarose with the attached 1D4 antibodies as described in [22]. The extent of purity of the purified preparations was determined by electrophoresis with the silver nitrate staining of polyacrylamide gels.

The purified protein (3 μL) was immediately loaded onto the mesh for electron microscopy, covered with carbon film for 30 s, the excess liquid was aspirated by filter paper, and 1% uranyl acetate solution (50 μL) was placed onto the drops for staining (2 times for 30 s).

Electron microscopy. Images were taken by electron microscope Tecnai G-12 (FEI, Netherlands) with acceleration voltage of 120 kV at the condition of low electron dose per square angstrom to prevent the sample damage by the electron beam. The images were taken using CCD camera Eagle (FEI, Netherlands) with magnification of 52000 and defocus 1.4–3 μm.

The image selection of separate molecules of ion channel proteins for further three-dimensional (3D) reconstruction was performed manually using Signature software [32]. The further processing was performed using IMAGIC software [20]; the standard

protocol described in [33] was used for this purpose. The selected images of separate channels were filtered from noise, normalized and center aligned by using image rotation, and their movement compared with the averaged image.

The following sequence of steps was used for image classification: (1) The aligned images were subjected to multivariant statistical analysis (MSA) [20, 21], where each image was presented as a point in a multidimensional space. MSA determines the new coordinate system, where each aligned image can be presented as a linear combination of independent images. (2) The images processed with the help of MSA were divided into classes. The channel images in one orientation were assigned to one class. (3) The best quality classes, comprised of multiple images, are used after as a reference point in the multireference analysis (MRA) [20]. Ten cycles of MRA, MSA and classification were conducted. (4) The obtained images were divided by the repeated cycles of MSA and classification. (5) The 3D structure of the channel was calculated using angle reconstruction [34] with supplementation of the four-sided symmetry [35]. (6) The reverse projections of the 3D-reconstruction were further used for the subsequent MRA. The stable classes were obtained after six iterations of alignment and reconstruction.

The resolution of the structure obtained was measured with the help of the Fourier shell correlation coefficient (FSC) [35], where the resolution limit is determined as a point with the FSC of 0.5 [36].

The production of fluorescently labeled agitoxin 2 for channel expression test. The correctness of folding of channels expressed in Vero cells was tested using the labeled ligand agitoxin 2. Plasmid vector *pCSP105* was kindly provided by K. Miller (Brandeis University, USA). Agitoxin expression and purification was conducted as described earlier in [24] with the changes described in [23].

Agitoxin was labeled with fluorescent dye Cy3 (GE Healthcare, USA) according to manufacturer's recommendations with minor changes. The Cy3 aliquot was dissolved in PBS buffer (pH 8.0), added to the protein solution and incubated overnight at +4°C. The excess of the unbound dye was removed using 3YM Microcon filter (Millipore).

To test the channel expression on the cell surface, the fluorescently labeled agitoxin (10 nM) was added directly to the nutrient medium with the serum, incubated for 30 min at +4°C followed by washing with the medium without serum.

Confocal microscopy. Digital images were obtained using LSM-510 Meta microscope (Carl Ziess AG, Germany). Images with resolution of 1024 × 1024 pixel were recorded using Plan-Apochromat 100×/1.4Oil Ph3. Helium-neon laser (emission wavelength 543 nm) was used for excitation of Cy3 label, a bandpass filter with the passband 565–615 nm was used for fluorescence registration. According to manufacturer's instructions, the diaphragm was set to 1.74 Airy units for the image acquisition with time resolution to increase focus depth in order to obtain images with high resolution. Zeiss LSM 510Meta, version 3.2 software was used for image processing.

Homology modeling. SWISS-MODEL server [37] was used to identify templates. The SWISS-MODEL search identified the most homologous templates for the Kv10.2 channel sequence in the structure database. The highest homology percent for the Kv10.2 channel corresponded to the Mloti1 structure (PBD ID: 2ZD9, C-subunit). Hence, the structure of the transmembrane part of cAMP-dependent bacterial channel MlotiK1 [38] (PBD ID 2ZD9, C-subunit) was chosen as a template for the construction of the model of the membrane part of Kv10.2 channel.

Amino acid sequences were aligned using T-COFFEE software [39]. The fragment 144–549 (with the exception of loops 64–150 and 349–402 that have weak homology with MlotiK1 structure) was isolated from the entire amino acid sequence of the Kv10.2 channel. Amino acids of the Kv10.2 channel from 12th to 90th and from 91st to 143rd were used for the model construction of the N-terminal domains of PAS and PAC, respectively. The homologous structure of the N-terminal domains of the human potassium channel *herg* (PBD ID: 2LOW, A subunit) was chosen as a template, a template search procedure was also performed through the SWISS-MODEL server [39].

For the C-terminal domain, the 550–667 fragment of the initial Kv10.2 channel sequence was aligned with the bacterial cAMP-dependent channel MloK1 (PBD ID: 2KXL) as a template. The model construction based on the alignment of the homologous amino acid sequences was conducted using MODELLER software [40].

Model of the quaternary structure was constructed with the symmetry matrix consideration in the UCSF Chimera software [29]. Parameters of the symmetry matrix in the pdb-file were selected in correspondence with proteins homologous the proteins with the PBD ID: 1ORQ (KvAP voltage-gated potassium channel), 3OTF (cAMP-dependent human channel HCN4–tetramer in complex with cAMP ligands). The model docking was performed in a semiautomatic mode using UCSF Chimera software [29].

ACKNOWLEDGMENTS

The authors are grateful to the corresponding member of the Russian Academy of Sciences A.N. Kisilev for the opportunity to use Tecnai G12 electron microscope, to Professor K. Miller for providing plasmid for agitoxin 2 expression, and to Associate Professor M.M. Moisenovich for the help in obtaining confocal images of cells labeled by agitoxin 2. This work was supported by the Seventh Framework

Program of the European Union (program EDICT, project no. 201924), the Russian Foundation for Fundamental Research (projects nos. 08-04-013448-a, 09-04-12146-ofi_m, 10-04-01182-a), and the Ministry of Education and Science of Russian Federation (State contracts nos. 14.740.11.0255 and 14.740.11.0760).

REFERENCES

1. Wray, D., *Eur. Biophys. J.*, 2009, vol. 38, pp. 285–292.
2. Pardo, L.A., Contreras-Jurado, C., Zientkowska, M., Alves, F., and Stuhmer, W., *J. Membr. Biol.*, 2005, vol. 205, pp. 115–124.
3. Doyle, D.A., Morais, Cabral, J., Pfuetzner, R.A., Kuo, A., Gulbis, J.M., Cohen, S.L., Chait, B.T., and MacKinnon, R., *Science*, 1998, vol. 280, pp. 69–77.
4. Kuo, A., Gulbis, J.M., Antcliff, J.F., Rahman, T., Lowe, E.D., Zimmer, J., Cuthbertson, J., Ashcroft, F.M., Ezaki, T., and Doyle, D.A., *Science*, 2003, vol. 300, pp. 1922–1926.
5. Long, S.B., Campbell, E.B., and Mackinnon, R., *Science*, 2005, vol. 309, pp. 897–903.
6. Miyazawa, A., Fujiyoshi, Y., and Unwin, N., *Nature*, 2003, vol. 23, pp. 949–955.
7. Kawate, T., Michel, J.C., Birdsong, W.T., and Gouaux, E., *Nature*, 2009, vol. 460, pp. 592–598.
8. Tao, X., Avalos, J.L., and Chen, J., MacKinnon R., *Science*, 2009, vol. 326, pp. 1668–1674.
9. Ujwal, R., Cascio, D., Colletier, J.P., Faham, S., Zhang, J., Toro, L., Ping, P., and Abramson, J., *Proc. Natl. Acad. Sci. USA*, 2008, vol. 105, pp. 17742–17747.
10. Jasti, J., Furukawa, H., Gonzales, E.B., and Gouaux, E., *Nature*, 2007, vol. 449, pp. 316–323.
11. Ju, M., Stevens, L., Leadbitter, E., and Wray, D., *J. Biol. Chem.*, 2003, vol. 278, pp. 12769–12778.
12. Pischalnikova, A.V. and Sokolova, O.S., *J. Neuroimmune. Pharmacol.*, 2009, vol. 4, pp. 71–82.
13. Ludwig, V., Martin, W.H., and Delbeke, D., *Clin. Nucl. Med.*, 2003, vol. 28, pp. 108–112.
14. Malin, S.A. and Nerbonne, J.M., *J. Neurosci.*, 2002, vol. 22, pp. 10094–10105.
15. Saganich, M.J., Machado, E., and Rudy, B., *J. Neurosci.*, 2001, vol. 21, pp. 4609–4624.
16. Camacho, J., *Cancer. Lett.*, 2006, vol. 233, pp. 1–9.
17. Conti, M., *J. Exp. Ther. Oncol.*, 2004, vol. 4, pp. 161–166.
18. Cabral, J.H.M., Lee, A., Cohen, S.L., Chait, B.T., Li, M., and Mackinnon, R., *Cell*, 1998, vol. 95, pp. 649–655.
19. Zagotta, W.N., Olivier, N.B., Black, K.D., Young, E.C., Olson, R., and Gouaux, E., *Nature*, 2003, vol. 425, pp. 200–205.
20. van Heel, M., *Ultramicroscopy*, 1987, vol. 21, pp. 111–123.
21. van Heel, M. and Frank, J., *Ultramicroscopy*, 1981, vol. 6, pp. 187–194.
22. Sokolova, O., Kolmakova-Partensky, L., and Grigorieff, N., *Structure*, 2001, vol. 9, pp. 215–220.
23. Karlova, M.G., Piscshalnikova, A.V., Ramonova, A.A., Moisenovich, M.M., Sokolova, O.S., and Shaitan, K.V., *Biophysics (Moscow)*, 2011, vol. 56, pp. 272–279.
24. Miller, C., *J. Gen. Physiol.*, 1988, vol. 91, pp. 335–349.
25. Napp, J., Monje, F., Stuhmer, W., and Pardo, L.A., *J. Biol. Chem.*, 2005, vol. 280, pp. 29506–29512.
26. Kim, L.A., Furst, J., Gutierrez, D., Butler, M.H., Xu, S., and Grigorieff, N., *Neuron*, 2004, vol. 4, pp. 513–519.
27. Sokolova, O., Accardi, A., Gutierrez, D., Lau, A., Rigney, M., and Grigorieff, N., *Proc. Natl. Acad. Sci. USA*, 2003, vol. 100, pp. 12607–12612.
28. Orlova, E.V., Papakosta, M., Booy, F.P., van Heel, M., and Dolly, J.O., *J. Mol. Biol.*, 2003, vol. 326, pp. 1005–1012.
29. Pettersen, E.F., Goddard, T.D., Huang, C.C., Couch, G.S., Greenblatt, D.M., Meng, E.C., and Ferrin, T.E., *J. Comput. Chem.*, 2004, vol. 25, pp. 1605–1612.
30. Sanguinetti, M.C. and Xu, Q.P., *J. Physiol.*, 1999, vol. 514 P, pp. 667–675.
31. Terlau, H., Heinemann, S.H., Stuhmer, W., Pongs, O., and Ludwig, J., *J. Physiol.,* 1997, vol. 502, pp. 537–543.
32. Chen, J.Z. and Grigorieff, N., *J. Struct. Biol.*, 2007, vol. 157, pp. 168–173.
33. Orlova, E.V. and van Heel, M., *J. Mol. Biol.*, 1997, vol. 271, pp. 417–437.
34. van Heel, M. and Stoffer-Meilicke, M., *EMBO J.*, 1985, vol. 4, pp. 2389–2395.
35. Harauz, G. and van Heel, M., *Optik*, 1986, vol. 73, pp. 146–156.
36. Bottcher, B., Kiselev, N.A., Stel'mashchuk, V.Y., Perevozchikova, N.A., Borisov, A.V., and Crowther, R.A., *J. Virol.*, 1997, vol. 7, pp. 325–330.
37. Kiefer, F., Arnold, K., Konzli, M., Bordoli, L., and Schwede, T., *Nucleic. Acids. Res.*, 2009, vol. 37, pp. D387–D392.
38. Clayton, G.M., Altieri, S., Heginbotham, L., Unger, V.M., and Morais-Cabral, J.H., *Proc. Natl. Acad. Sci. U. S. A.*, 2008, vol. 105, pp. 1511–1515.
39. Notredame, C., Higgins, D.G., and Heringa, J., *J. Mol. Biol.*, 2000, vol. 302, pp. 205–217.
40. Eswar, N., Marti-Renom, M.A., Webb, B., Madhusudhan, M.S., Eramian, D., Shen, M., Pieper, U., and Sali, A., *Curr. Protocols Bioinform.*, 2006, Oct. U. 5.6.1–5.6.30.